Study of the Interaction between a Shock Wave and a Cloud of Droplets

A. Chauvin, G. Jourdan, E. Daniel, L. Houas, and R. Tosello

1 Introduction

The pressure histories obtained when a shock wave propagates into an air-solid particle medium is well known: the overpressure jump decreases, as the shock wave propagates into the mixture and is followed by a pressure build-up corresponding to the velocity relaxation processes. In the present paper, an air-water droplet mixture interacting with a shock wave has been studied and the comportment of the pressure traces was found significantly changed in comparison to the interaction with a air-solid particle mixture. This is attributed to the ability of the droplets to deform and fragment into finer ones. This phenomenon, known as secondary atomisation, widely reviewed by Gelfand[1] and by Guildenbecher[2], affects both the pressure histories and the impulse induced by the shock wave. We have previously studied the influence of the height of cloud of droplets on shock wave propagation [3]. In the present work, we focus our attention on the influence of the droplet diameter on the attenuation of shock wave propagating into the air-water mixture. Moreover, predictions obtained by 1D numerical simulations are compared to the experimental results. The necessity to introduce a secondary atomisation model to fit the experimental behaviour is then underlined.

2 Experimental Set-Up

Experiments were carried out in the T80 shock tube of the IUSTI laboratory, oriented in vertical position. It consists in a 750 mm driver section followed by a 3045 mm driven section which includes a 880 mm plexiglass windows allowing the flow visualisation. A generator of mono-dispersed cloud of droplets was fitted

A. Chauvin · G. Jourdan · E. Daniel · L. Houas
IUSTI-CNRS, Aix-Marseille Université, 5 rue Enrico Fermi, Marseille, 13013, France

R. Tosello
DGA/TN, Avenue de la Tour Royale, Toulon, 83050, France

at the top of the experimental chamber [4], and released downward the air-water mixture characterized by a dispersion of $\sigma = 25\%$ on the mean diameter. The interaction between the cloud of droplets falling downward, and the shock wave propagating upward, was visualized by a high speed direct shadowgraphy system. It includes a Photron FastCam SA1 recording the pictures at an acquisition frequency of 15,000 frames per second with a spatial resolution of 128×864 pixels. For each run, pressure histories were recorded by two and eight PCB pressure transducers (SM113A26 type), located in the driver and the driven sections, respectively. Thus, a map of the pressure evolutions alongside the shock tube and the displacement of the droplet cloud was obtained both qualitatively and quantitatively. The experimental apparatus scheme is presented in Fig. 1 with gauge localisations.

3 Experimental Results

Two drilled grid are used in the cloud generator in order to study the influence of the droplet diameter on two shock wave Mach numbers of $M_{is} = 1.3$ and $M_{is} = 1.5$. The cloud of droplets is characterized by the mean diameter of its droplets, ϕ_d, its height, H_d and its volume fraction, α_d, defined by $\alpha_d = \frac{V_d}{a^2 H_d}$, where V_d is the volume of discharged water . Note that the clouds, composed by droplets of 250 μm and 500 μm in diameter, have a volume fraction of 0.3% and 1%, respectively.

The mean height of the clouds is maintained approximatively constant for the two cases (781 mm $\pm 15\%$), due to the reaction time of the droplet generator. Fig. 1 presents the behaviour of a cloud of 768 mm in height, composed by droplets of 250 μm in diameter, interacting with a $M_{is} = 1.5$ shock wave Mach number. The six lines drawn correspond to the six pressure measurement stations located in the test section. Time in milliseconds indicated at the bottom of the pictures, corresponds to the time elapsed since the shock wave passed at station S_8. From the first picture, showing the two-phase medium before the shock wave impacts it (t_1), the height of the air-water mixture, H_d, and the abscissa of the interaction, X_{int}, are determined. Then, the shock wave propagating in ambient air impacts the water droplet cloud, of higher density. Consequently, a part of the shock wave is transmitted into the air-water mixture whereas an other part is reflected and propagates upstream. The arrow in Fig. 1 indicates the position of the incident (t_1) and transmitted shock wave (t_2 and t_3). As the shock wave penetrates into the two-phase mixture, the droplets are atomised into smaller ones. This phenomenon, known as secondary atomisation, is well observable at t_2. The fragmentation regimes which occurs during this study corresponds to the regime II described by Gelfand [1]. Pilch and Erdman [5] estimated the fragmentation time τ_{frag} required to atomise a droplet into smaller droplets of stable diameter ϕ_f. In Fig. 1, a delay between the observation of the shock wave and the secondary atomisation front is detected. It corresponds to the distance required for a droplet to deform and atomise. From t_2 to t_6, the momentum transfer from the shock wave to the cloud is observable by its displacement. It is one of the attenuation process with the heat transfer and atomisation phenomenon. Fig. 2 presents the pressure histories obtained at four stations (S_8, S_6, S_5 and S_2)

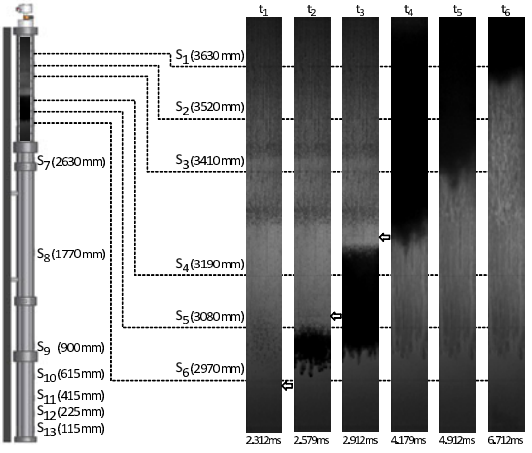

Fig. 1 Sequence of shadowgraph pictures showing the interaction of a planar shock wave of Mach number M_{is}=1.5 moving upwards with a cloud of droplets of 250 μm in diameter and 768 mm in height falling downwards (T80#711), where labels denote exposure timings in milliseconds relative to the shock passage at station S_8

during the interaction of a $M_{is} = 1.3$ shock wave and two water clouds composed by droplets of 250 μm and 500 μm in diameter. They are compared with pressure traces obtained in absence of two-phase mixture. At station S_8, typical pressure histories induced by a shock wave is observed until the arrival of the reflected one by the air-water mixture. We can note that this reflection is smaller than the one coming from a rigid wall and is weaker for the cloud containing the finer droplets (250 μm). The interaction abscissa, X_{int}, of the two clouds composed by 250 μm and 500 μm are respectively of 2873 mm and 2934 mm. Thus, just after the interaction location, station S_6, the pressure increases after the passage of the transmitted shock wave for the two clouds. Finally, the pressure reaches an equilibrium value corresponding to the one induced by the reflected shock wave. As the transmitted shock wave propagates into the water cloud, from stations S_5 to S_2, the frozen pressure jump decays, as observed during the interaction of shock wave with a solid-particle mixture [6]. Nevertheless, in the presence of liquid droplets, this overpressure peak is followed by a rarefaction zone which can be attributed to the capability of droplets to deform and fragment. Therefore, the exchange surface area increases and leads to the augmentation of the transfer between the two media, which will extract energy from the shock wave. As the exchange surface area increases, the flow slows down which causes this rarefaction zone. Afterwards, a pressure build-up occurs, due to the velocity relaxation process. Thus, the droplets are transported to reach the flow velocity which leads to an equilibrium pressure value. Finally, the cloud composed by higher diameter droplets induces a softer pressure evolution than the other cloud, constituted by the 250 μm droplets. It may be linked to the volume fraction three time smaller for the cloud containing the droplets of 250 μm in diameter. The overpressure peak measured just behind the shock wave in presence of a droplet cloud

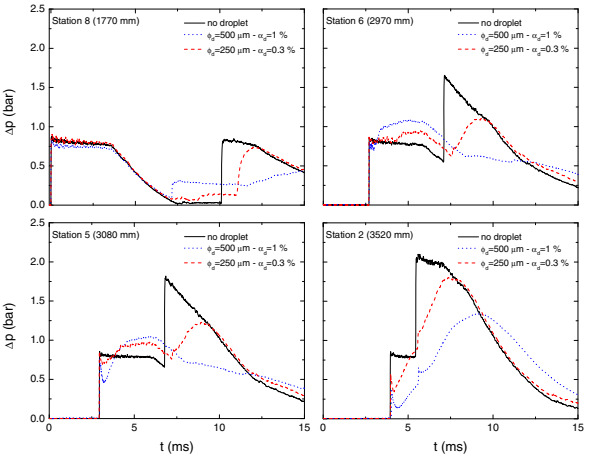

Fig. 2 Comparison of pressure histories obtained with a shock wave of $M_{is} = 1.3$ Mach number, at the stations S_8, S_6, S_5 and S_2, during runs without droplet and with clouds of droplets of 250 μm and 500 μm in diameter with a volume fraction of 0.3% and 1%, respectively

ΔP^{shock} was non-dimensionnalized by the overpressure peak obtained just behind the shock wave without cloud of droplets ΔP_0^{shock} to compare the attenuation capability of the different clouds. The ratio $\frac{\Delta P^{shock}}{\Delta P_0^{shock}}$ versus the position of the shock wave since it encountered the air-water mixture, $X - X_{int}$, non dimentionnalized by the height of the cloud, H_d, is represented in Fig. 3 at each station of measurement X. Note that $\frac{X - X_{int}}{H_d} = 1$ corresponds to the end of the droplet cloud. As we can see from this representation, the overpressure mitigation $(1 - \frac{\Delta P^{shock}}{\Delta P_0^{shock}})$ increases with the shock wave Mach number and the droplet mean diameter.

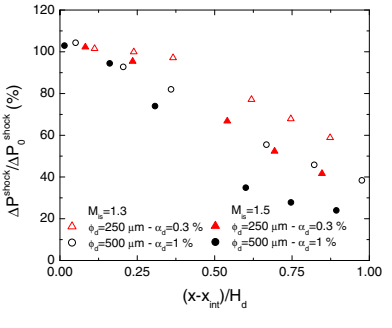

Fig. 3 Attenuation of the overpressure peak behind the transmitted shock front in presence of clouds of droplets for the different cases studied, versus its distance of propagation in the two-phase mixture non-dimensionalized by the height of the cloud. X is the sensor location

Nevertheless, note that the volume fraction is divided by three for the smaller diameter. Therefore, the cloud composed by the 250 μm droplets seems to be more effective to mitigate the shock wave as regards to the volume fractions. Finally, in our experimental conditions, the mitigation of the overpressure peak induced by a shock wave passing through a water cloud can reach up to 80%.

4 Numerical Results

One dimensional unsteady calculations were performed in order to improve the knowledge on the air-water mixture shock wave interaction. Thus, the droplets cloud was approached by a classical two-phase-dilute flows[7], using a Eulerian/Eulerian mathematical model. The drag force, the heat transfer between the air-water mixture and the flow have been taken into account. The droplets are assumed as spherical at uniform temperature. The gas is governed by the Euler equations and the droplet phase by its specific set of partial differential equations [4]. The dispersed phase and the gas phase are coupled by interaction terms. Moreover, a secondary atomisation model of the droplets is introduced. Fig. 4 represents the experimental pressure history obtained at station S_1 for clouds of 500 μm or 250 μm impacted by a M_{is}=1.5 shock wave compared with numerical results. As we can see, if the droplet fragmentation is not taken into account, the computational pressure trace does not fit to the experimental one. This result emphasis the predominant role of the secondary atomisation on the pressure history behaviour. Consequently, we added a source term of droplet production to the equation on the number of droplets per unit volume, which becomes:

$$\frac{\partial n_d}{\partial t} + \frac{\partial (n_d u_d)}{\partial x} = \dot{n_d} \quad with \quad \dot{n_d} = \left(\left(\frac{\phi_d}{\phi_f} \right)^3 - 1 \right) \frac{n_d}{\tau_{frag}} \tag{1}$$

where n_d and u_d are respectively the number and the velocity of the dispersed phase and τ_{frag} is the time, defined in [5], required to reach the final fragmentation of the droplets.

Nevertheless, Fig. 1 shows that the secondary atomisation front is delayed compared to the shock front. Thus, to consider this time, τ, when the flow and the air-water mixture are in unstable conditions, another partial equation is written to delay the initiation of the fragmentation :

$$\frac{\partial \tau}{\partial t} + u_d \frac{\partial \tau}{\partial x} = \dot{\tau} \tag{2}$$

where τ measures the time in order to obtain the total time of breakup, taken from Pilch and Erdman [5], including a delay due to unstable conditions.

Finally the computational results obtained when the secondary atomisation stages of the droplets are considered, give a behaviour closer to the experimental results, as shown in Fig. 4.

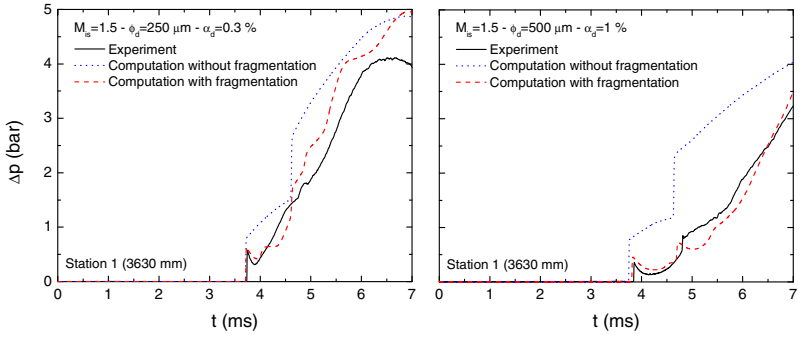

Fig. 4 Experimental pressure histories recorded at the station S_1, for two droplets mean diameter (250 μm and 500 μm) impacted by a $M_{is} = 1.5$ shock wave and compared to the computational pressure trace obtained with and without secondary atomisation model.

5 Conclusion

The present experimental investigation on the influence of the mean diameter of the droplets on the attenuation of shock waves highlighted the major role of the exchange surface. Indeed, the momentum transfer and heat exchange which absorb energy from the shock wave depends on the exchange surface area. The attenuation of the shock wave increases with the Mach number and the droplet diameter studied. Nevertheless, due to our experimental device, the volume fraction was three time higher for the cloud composed by the droplets of $\phi_d = 500\ \mu m$ in diameter. Future study focusing the influence of the volume fraction, maintaining a constant mean diameter are envisaged. It will allow to have a better understanding on the weight of the volume fraction on the shock wave attenuation. Moreover, numerical simulations were carried out and a good agreement with our experimental results is found, particularly, if the fragmentation of droplets is taken into account in the model.

References

1. Gelfand, B.E.: Prog. Energy Comb. 22, 3 (1996)
2. Guildenbecher, D.R., López-Rivera, Sojka, P.E.: Exp. Fluids 46, 3 (2009)
3. Chauvin, A., Zerbib, J., Jourdan, G., Daniel, E., Mariani, C., Houas, L., Biamino, L., Tosello, R., Praguine, D.: Proccedings of the 21th MABS Symposium, Jerusalem (October 2010)
4. Jourdan, G., Biamino, L., Mariani, C., Blanchot, C., Daniel, E., Massoni, J., Houas, L., Tosello, R., Praguine, D.: Shock Waves 20, 4 (2010)
5. Pilch, M., Erdman, C.A.: Int. J. Mult. Flow 13, 6 (1987)
6. Sommerfeld, M.: Experiments in Fluids 3, 4 (1985)
7. Daniel, E., Saurel, R., Larini, M., Loraud, J.-C.: Int. J. Heat and Fluid Flow 4, 3 (1994)